Journal of Information Technology and Digital World (ISSN: 2582-418X)
www.irojournals.com/itdw/

Smart Home Energy Digital Twin with Agentic Optimisation Control

Kavindu Karunarathne

Department of Computer and Data Science, York St John University, London, United Kingdom

E-mail: k.karunarathne@yorksj.ac.uk

Abstract

Dynamic time-of-use electricity tariffs expose households to half-hourly price volatility, yet most domestic loads and battery systems are still operated on static schedules that ignore this signal. This research presents a smart home energy digital twin that couples real half-hourly tariff data from the Octopus Energy Agile API with historical solar radiation data from Open-Meteo, a physics-informed home battery model incorporating charge and discharge efficiency and an explicit cycling degradation cost, and a deferrable appliance load. Three autonomous control strategies are evaluated within the digital twin: a static baseline controller; a forecast-aware agent that applies interpretable price look-ahead rules for battery arbitrage and appliance scheduling; and a mixed-integer linear programming (MILP) optimiser that computes a cost-minimal 24-hour schedule subject to battery dynamics, energy-balance, and appliance-deadline constraints. A 30-day backtest over December 2024, selected as a deliberately adverse low-solar and high-volatility stress period, shows that the forecast-aware agent reduces the effective energy cost by 21.41% (£28.20) relative to the baseline, while the MILP optimiser achieves a 27.71% reduction (£36.50) and is cheaper on every one of the 30 days. An analytical derivation and a sensitivity analysis confirm that the agent's decision thresholds are economically grounded and that its performance is robust across wide threshold ranges. Notably, the optimiser attains the lowest cost while importing slightly more grid energy, demonstrating that intelligent load shifting into low-price windows, rather than import minimisation, drives cost reduction under dynamic pricing.

Keywords: Digital Twin; Smart Home Energy Management; Mixed-Integer Linear Programming; Battery Scheduling; Time-of-use Tariff; Agentic Control; Solar Photovoltaics.

Journal of Information Technology and Digital World, September 2026, Volume 8, Issue 3, Pages 269-286
DOI: https://doi.org/10.36548/jitdw.2026.3.010
Received: 26.06.2026, received in revised form: 30.07.2026, accepted: 16.08.2026, published: 28.08.2026

1. Introduction

The decarbonization of electricity systems has involved significant levels of variability in renewable energy generation sources and thereby volatility in electricity prices which can be directly transferred to consumers through time-of-use tariffs. The Octopus Agile tariff in the UK announces its half-hourly electricity import prices one day in advance. Prices are regularly highly volatile with daily price ratios often exceeding a factor of three and sometimes even going negative in days with an oversupply of wind generation. Such price information presents a potentially large saving opportunity for the owner of a house that has rooftop photovoltaic panels (PV), a battery storage system, and flexible loads, but cannot be exploited by humans in practice.

Digital twin technology offers a principled route to this problem. A digital twin is a virtual replica of a physical system that is synchronised with real operating data and used for monitoring, prediction, and control evaluation [1][2][3]. In the residential energy context, a digital twin allows candidate control policies to be tested safely and repeatably against real tariff and weather conditions before they are entrusted with a physical battery and real money. When such a twin is coupled with software agents that autonomously perceive system state, reason over available forecasts, and act on the environment, it becomes an operational decision-making platform rather than a passive model; in this study, this combination is referred to as agentic control.

The *digital twin* denotes the virtual household model (demand, solar PV, and battery) synchronised with real tariff and solar data. The *forecast-aware agent* denotes the rule-based control strategy that uses price look-ahead. The *MILP optimiser* denotes the mathematical-optimisation control strategy. *Agentic control* is used only as the umbrella term for the two autonomous strategies collectively.

Current study makes three contributions:

- Presents an end-to-end smart home energy digital twin driven entirely by real data: half-hourly Agile tariff prices retrieved from the Octopus Energy public REST API and household solar generation derived from Open-Meteo historical shortwave radiation for Cardiff, UK. The digital twin models a 5 kWh home battery with 95% charge and discharge efficiency and an explicit cycling degradation cost, a time-varying household demand profile, and a deferrable washing machine load.

- Implements and compares three autonomous control strategies of increasing sophistication: a static baseline, the forecast-aware agent, and the MILP optimiser, with the agent's decision thresholds derived analytically from battery economics and validated through sensitivity analysis.
- Reports a rigorous 30-day backtest (1–30 December 2024) with a continuous battery state of charge carried across days, quantifying the cost, grid-import, and battery-behaviour differences between the strategies. Analysis leads to an important conclusion that the most economical method is not that which brings in the lowest quantity of energy, but that which purchases energy at the appropriate time.

The remainder of the paper is organised as follows. Section 2 reviews and compares related work. Section 3 describes the system architecture, the digital twin model, and the three control strategies, including the threshold derivation. Section 4 details the experimental setup and its justification. Section 5 presents the backtest results, the sensitivity analysis, and a discussion of limitations, and Section 6 concludes with directions for future work.

2. Related Works

A lot of research has been carried out on home energy management systems (HEMS). Beaudin and Zareipour [4] reviewed the modeling options and complexities involved in HEMS modeling, Zhou et al. [5] categorized different HEMS architectures and scheduling methods, and Mahapatra and Nayyar [6] gave an overview of HEMS. In the case of optimization-based scheduling algorithms, Mohsenian-Rad and Leon-Garcia [7] presented optimal control of residential loads based on real-time pricing and price prediction, Chen et al. [8] generalized the price based demand response scheduling to stochastic and robust cases, and Sou et al. [9] modelled appliance scheduling as a mixed integer programming problem. A parallel thread applies learning-based agents: O'Neill et al. [10] introduced reinforcement learning (RL) for residential demand response, Vázquez-Canteli and Nagy [11] review RL algorithms and modelling techniques for demand response, and Yu et al. [12] apply deep RL to smart home energy management. Digital twin concepts originating in manufacturing [1]–[3] have more recently been transferred to the built environment: Agostinelli et al. [13] combine digital twins with artificial intelligence for building energy management, Onile et al. [14] review digital twin applications for energy services and demand-side management, and O'Dwyer et al. [15] position such cyber-physical energy systems in the smart-city context.

Table 1 compares these strands of work against the present study along the dimensions most relevant to practical deployment: the realism of the price signal, solution optimality, interpretability, treatment of battery degradation, and whether competing control paradigms are benchmarked within one real-data environment.

Table 1. Comparison of the proposed work with existing HEMS, optimisation, reinforcement-learning, and digital twin approaches.

Approach	Representative Studies	Key Strengths	Key Limitations
Heuristic / rule-based HEMS	Zhou et al. [5]; Mahapatra and Nayyar [6]	Simple, interpretable, cheap to deploy	No optimality guarantee; thresholds often ad hoc and unjustified
Optimisation-based scheduling (LP/MILP)	Mohsenian-Rad and Leon-Garcia [7]; Chen et al. [8]; Sou et al. [9]	Exact cost-optimal schedules; constraints handled explicitly	Often evaluated on synthetic or averaged prices; degradation frequently omitted
Reinforcement learning control	O'Neill et al. [10]; Vázquez-Canteli and Nagy [11]; Yu et al. [12]	Model-free; adapts to uncertainty	Sample-inefficient; opaque policies; performance hard to verify before deployment
Digital twin energy platforms	Agostinelli et al. [13]; Onile et al. [14]	Safe policy evaluation on synchronised real data	Mostly monitoring-oriented; rarely benchmark multiple control paradigms head-to-head
Proposed work	—	Real Agile tariff and solar data; baseline, rule-based, and MILP strategies benchmarked in one twin; degradation costed; thresholds derived and sensitivity-tested	Single-region, single-month evaluation; perfect day-ahead foresight (see Section 5.5)

Three key gaps arise from this contrast, motivating the current study. Firstly, most of the literature focuses on the evaluation of one particular control strategy in isolation, making it hard to estimate how much of the achievable saving the basic interpretable model already achieves compared to the exact optimization, where both are evaluated against the same inputs. Secondly, numerous studies employ some artificially generated or averaged prices instead of real fluctuating half-hourly prices currently available on the market; in the current research, the actual Agile price is used for all experiments. Thirdly, battery wear-and-tear costs are often left out of the objectives, resulting in an inflation of savings due to the encouragement of free battery cycling.

3. System Architecture and Methodology

Figure 1 shows the overall architecture, real data flow from two public APIs into the digital twin, which maintains the household state at half-hourly resolution. Each control strategy observes the same twin state and the same price and solar series, issues battery and appliance actions, and the resulting costs are accumulated for comparison.

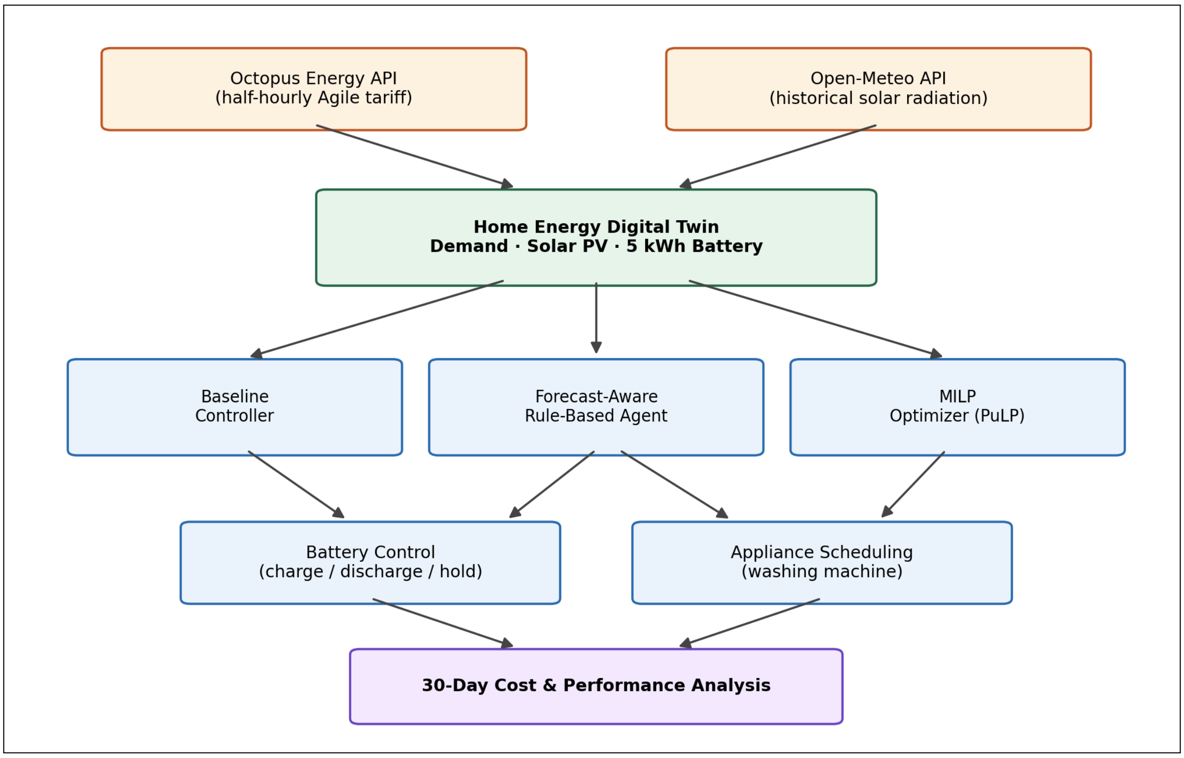

Figure 1. System architecture of the smart home energy digital twin with three control strategies.

3.1 Real Data Acquisition

Tariff data. Half-hourly import prices (pence/kWh, including VAT) are retrieved from the Octopus Energy public REST API [17] for the Agile product AGILE-FLEX-22-11-25, regional tariff code E-1R-AGILE-FLEX-22-11-25-C (South Wales). It is emphasised that the date embedded in an Octopus product code denotes the product's launch date, not the data period: AGILE-FLEX-22-11-25 is the product "Agile Octopus November 2022 v1", launched on 25 November 2022 and still active throughout the study period (the API reports available_to = null). The API publishes the complete history of half-hourly unit rates for an active product, and any calendar window can be requested through the period_from and period_to parameters [17]. For each simulated day, exactly one UTC calendar day (48 intervals) of December 2024 rates was fetched under this product, sorted oldest-first, and validated for completeness so that the twin's 00:00–23:30 timeline aligns with the tariff timeline.

Solar data. Historical hourly shortwave radiation (W/m²) for Cardiff (51.48°N, 3.18°W) is retrieved from the Open-Meteo archive API [18] and converted to PV energy assuming a 20 m² array at 20% panel efficiency:

$$E_{\text{solar}}\,(\text{kWh}) = G\,(\text{W/m}^2) \times A\,(\text{m}^2) \times \eta_{\text{panel}}/1000 \tag{1}$$

where G is the hourly mean irradiance, A the array area, and _panel the panel efficiency. Because the archive provides hourly values while the twin operates at 30-minute resolution, each hourly energy value is divided equally across its two constituent half-hour intervals. Three considerations justify this choice. First, the transformation is exactly energy-conserving: daily and hourly PV energy totals, which dominate the cost calculation, are unaffected, and only the sub-hourly placement of energy is approximated. Second, all three control strategies receive the identical solar series, so the paired comparison between strategies, which is the object of this study, is unaffected by the interpolation method. Third, an upper bound on the resulting distortion is small: even if intra-hour generation were maximally skewed, at most half of one hour's energy (0.42 kWh on the sunniest December day) could be displaced by 30 minutes, corresponding to a worst-case cost perturbation well below 1% of the daily bill at typical intra-hour price differences. Sub-hourly satellite-derived irradiance will nevertheless be adopted in future work, as noted in Section 6. December conditions produced between 1.08 and 4.20 kWh of solar generation per day (mean 2.31 kWh), totalling 69.23 kWh over the backtest (Figure 2).

3.2 Digital Twin and Battery Model

The digital twin maintains the household state: instantaneous demand, solar generation, grid import, and the battery state of charge (SOC). Household base demand follows a stylised occupancy profile with a morning peak (0.55 kWh per interval, 06:00–09:00), an evening peak (0.75 kWh, 16:00–21:00), and lower overnight and daytime levels. A deferrable washing machine consumes 1.2 kWh in a single interval and must run once per day within an 08:00–20:00 window.

The battery is modelled with asymmetric conversion losses. Charging with an external energy c stores c · c in the battery; delivering an external energy d removes d / d from the battery, with c = d = 0.95. The SOC therefore evolves as:

$$SOC(t+1) = SOC(t) + \eta_c \cdot c(t) - d(t)/\eta_d \tag{2}$$

subject to 0 SOC(t) 5 kWh and per-interval limits c(t), d(t) 1 kWh. Battery ageing is represented by a linear throughput cost: every kWh of energy that passes through the battery in either direction, measured on the external (AC) side, incurs a degradation charge of = 1 p/kWh. The cumulative degradation cost of a strategy is therefore:

$$C_{deg} = \delta \cdot \sum_t [c(t) + d(t)] \tag{3}$$

and is added to the grid energy cost to form the effective cost on which all strategies are compared. This prevents any controller from treating battery cycling as free and makes the reported savings conservative. Table 2 summarises all model parameters.

Table 2. Simulation and backtest parameters.

Parameter	Value
Scheduling horizon	24 h (48 half-hourly intervals)
Battery capacity	5.0 kWh
Maximum charge / discharge per interval	1.0 kWh

Charge efficiency (η_c)	95%
Discharge efficiency (η_d)	95%
Battery degradation cost (δ)	1.0 p per kWh of throughput
Washing machine load	1.2 kWh (single interval, 08:00–20:00 window)
Solar array (Open-Meteo conversion)	20 m^2, 20% panel efficiency
Tariff	Octopus Agile (AGILE-FLEX-22-11-25, region C)
Backtest period	1–30 December 2024 (Cardiff, UK: 51.48°N, 3.18°W)

3.3 Baseline Controller

The baseline represents a non-smart household: the washing machine always runs at 08:00, solar generation is consumed opportunistically, the battery is not actively cycled against the tariff, and all residual demand is met by grid import at the prevailing Agile price. Its effective cost is almost entirely energy cost (£131.61 of £131.74 over the backtest).

3.4 Forecast-Aware Agent

The forecast-aware agent embodies a transparent, interpretable decision policy that exploits the day-ahead visibility of Agile prices. For appliance scheduling, it scores every feasible interval by score = price 10 × solar and selects the minimum, jointly preferring low-price periods and high solar availability. For battery control, at each interval t it examines a 4-hour look-ahead window (8 intervals) of future prices with average p, maximum p_max, and current price p(t), and applies three rules: (i) charge when the battery has headroom, p(t) < · p, and p_max > · p(t), i.e., energy is cheap now and substantially more expensive energy is imminent; (ii) discharge when p(t) > · p; and (iii) after 21:00, discharge any SOC above the 2.5 kWh end-of-day target so that value is not stranded overnight. Otherwise the battery holds. The selected values are = 0.70, = 1.40, and = 1.25.

3.5 Threshold Derivation

The thresholds are not arbitrary: they follow from the arbitrage economics of the modelled battery. A grid-to-battery-to-load cycle purchases E kWh at buy price p_b, incurring cost p_b · E plus charge degradation E; the stored c · E later delivers c · d · E = 0.9025E to the load, avoiding purchase at sell-time price p_s and incurring discharge degradation · 0.9025E. The cycle is profitable only when:

$$\frac{p_s}{p_b} > \frac{p_b + \delta(1+\eta_c\eta_d)}{\eta_c\eta_d\, p_b} = \frac{1}{\eta_c\eta_d} + \frac{\delta(1+\eta_c\eta_d)}{\eta_c\eta_d\, p_b}. \tag{4}$$

Given the average realized import price of 23.44 p/kWh in December 2024, Equation (4) yields the price ratio at which breakeven occurs as 1.198. The spread requirement = 1.40 imposes a breakeven ratio as well as a safety margin of about 17% to cushion from any instances where price peaks may not materialize during the look-ahead period. The charging ratio = 0.70 ensures that the energy stored is bought from the cheapest price range and not just below the average price, while the discharge ratio = 1.25 ensures that the energy is discharged only when the price is higher than the breakeven price.

3.6 MILP Optimiser

The MILP optimizer generates an exact schedule with minimum cost for every day using the PuLP library [16] along with the CBC solver. Decision variables corresponding to interval t {0, . . . , 47} are grid consumption g(t), solar export x(t), battery charging c(t) and discharging d(t), a binary variable m(t) which ensures exclusive charging or discharging but not both simultaneously, and a binary variable indicating washing machine usage w(t). The objective minimises the total effective cost:

$$\min \sum_t [g(t)\cdot\pi(t)] + C_{\text{deg}} \tag{5}$$

where (t) is the Agile price and C_deg is given by Equation (3), subject to: the SOC dynamics of Equation (2) with bounds; the mode constraints c(t) c_max · m(t) and d(t) d_max · (1 m(t)); the per-interval energy balance

$$g(t) + s(t) + d(t) = b(t) + 1.2\cdot w(t) + c(t) + x(t) \tag{6}$$

with s(t) the solar generation and b(t) the base demand; the export cap x(t) s(t); and the appliance constraint t w(t) = 1 restricted to the 08:00–20:00 window. The SOC at the beginning of the day is bound to be equal to the SOC at the end of the previous day, while the end-of-day SOC is kept unconstrained, letting the optimisation determine how many kWh to store. Each single problem instance (around 290 variables, where 96 are binary) can be solved in a fraction of a second.

4. Experimental Setup

Each of the strategies was back-tested during a 30-day period in December 2024 using exactly the same input data for all of them – the same actual series of Agile prices, the same series of Open-Meteo-generated solar power, and the same demand pattern for each of the days. The battery SOC value is passed from one day to another in each strategy separately, so none of the strategies have any advantages due to artificial resetting to zero in the night time.

The use of December as the only month for backtesting deserves special justification. December was chosen as a stress month on purpose because it has the lowest solar generation in a year, high winter tariffs and high evening demand, so the savings can be achieved only through smart time management. All strategies are evaluated in a paired design on identical inputs, the strict daily dominance ordering reported in Section 5 (optimiser < agent < baseline on all 30 of 30 days) is a property of the control logic under real winter conditions, and there is no mechanism by which higher-solar seasons would invert it; greater PV availability enlarges the feasible action space of the intelligent strategies relative to the baseline. What the single-month window cannot establish is the annualised magnitude of the savings, which will vary with season, and the export economics of summer surpluses. Accordingly, the reported percentages are presented as winter stress-test results, this scoping is acknowledged as a limitation in Section 5.5, and a full-year backtest is identified as future work in Section 6.

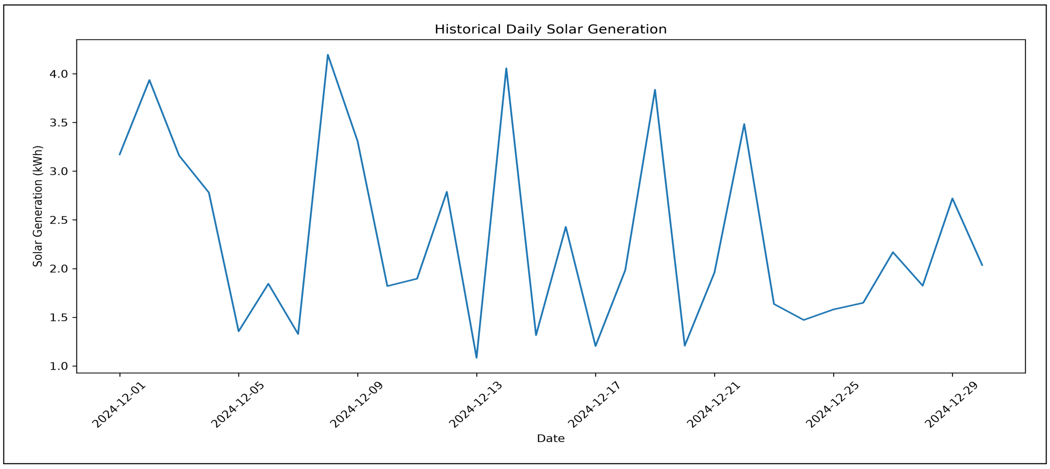

Figure 2. Historical daily solar generation for cardiff, December 2024 (Open-Meteo derived).

5. Results and Discussion

5.1 Aggregate Cost Performance

Table 3 summarises the 30-day totals. The percentage savings are computed relative to the baseline effective cost as:

$$Saving_s(\%) = \frac{C_{\text{baseline}} - C_s}{C_{\text{baseline}}} \times 100 \tag{7}$$

where C_s is the total effective cost (energy plus degradation) of strategy s. The baseline incurred C_baseline = £131.74. The forecast-aware agent reduced this to £103.53, giving (131.74 103.53) / 131.74 × 100 = 21.41% (£28.20), and the MILP optimiser to £95.24, giving (131.74 95.24) / 131.74 × 100 = 27.71% (£36.50). Both intelligent strategies were cheaper than the baseline on all 30 days, and the optimiser was additionally cheaper than the agent on all 30 days, confirming a strict and consistent performance ordering rather than an artefact of a few favourable days.

Table 3. Performance comparison of the baseline, forecast-aware agent, and MILP optimiser.

Metric	Baseline	Forecast Agent	MILP Optimiser
Grid energy cost (£)	131.61	100.73	91.54
Battery throughput (kWh)	12.5	280.1	369.9
Battery degradation cost (£)	0.12	2.80	3.70
Total effective cost (£)	131.74	103.53	95.24
Saving vs baseline (£)	—	28.20	36.50
Saving vs baseline (%)	—	21.41%	27.71%
Total grid import (kWh)	561.4	576.9	579.7
Days cheaper than baseline	—	30 / 30	30 / 30

The degradation entries in Table 3 follow directly from Equation (3). Over the 30 days, the baseline cycled only 12.5 kWh through the battery (opportunistic solar absorption), giving C_deg = 1 p/kWh × 12.5 kWh = 12.5 p £0.12. The forecast-aware agent cycled 280.1 kWh (£2.80) and the MILP optimiser 369.9 kWh (£3.70). The optimiser accepts the highest degradation cost because it cycles the battery whenever the price spread justifies it, yet still achieves the lowest total cost: the £40.07 of energy-cost saving it generates far exceeds the £3.58 of additional degradation it incurs relative to the baseline. Including degradation in the objective is nevertheless essential; without it, both intelligent strategies would over-cycle the battery and their real-world savings would be overstated.

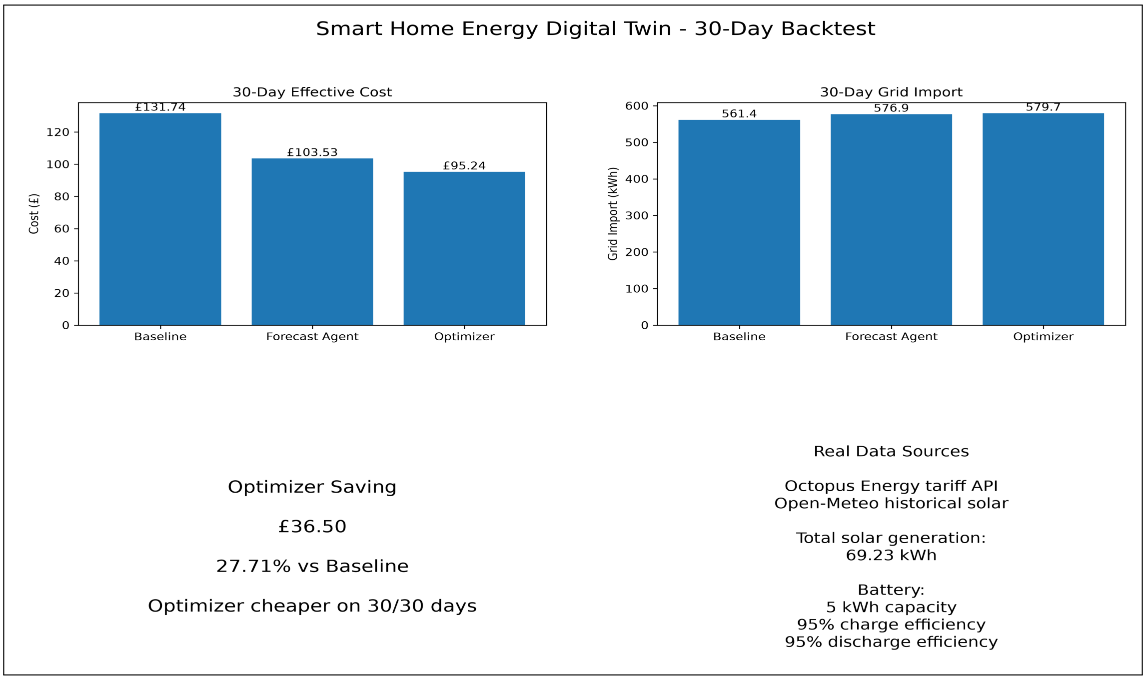

Figure 3. 30-day backtest summary: effective cost and grid import by strategy.

5.2 Daily Behaviour

Figure 4 plots the daily effective cost of the three strategies, and Figure 5 the optimiser's daily saving. The strategy ordering (baseline > agent > optimiser) holds on every day. Savings are strongly price-regime dependent: the largest optimiser saving, £3.57, occurred on 12 December, the most expensive and volatile day of the month (baseline cost £9.87), when wide intra-day spreads created substantial arbitrage and load-shifting value. Conversely, the smallest saving, £0.57 on 14 December, coincided with a flat, cheap tariff day on which even an exact optimiser has little price structure to exploit. Mean daily savings were £0.94 (agent) and £1.22 (optimiser), and both intelligent strategies also reduced the volatility of the household's daily bill, with the standard deviation of daily cost falling from £1.69 (baseline) to £1.32 (optimiser), as shown in Table 4. This implies a secondary benefit: hedging the household against tariff spikes.

Table 4. Daily cost statistics for the baseline, forecast-aware agent, and MILP optimiser.

Daily Statistic (£/day)	Baseline	Forecast Agent	MILP Optimiser
Mean daily cost	4.39	3.45	3.17
Standard deviation of daily cost	1.69	1.38	1.32
Mean daily saving vs baseline	—	0.94	1.22
Minimum daily saving	—	0.14	0.57
Maximum daily saving	—	3.03	3.57 (12 Dec)

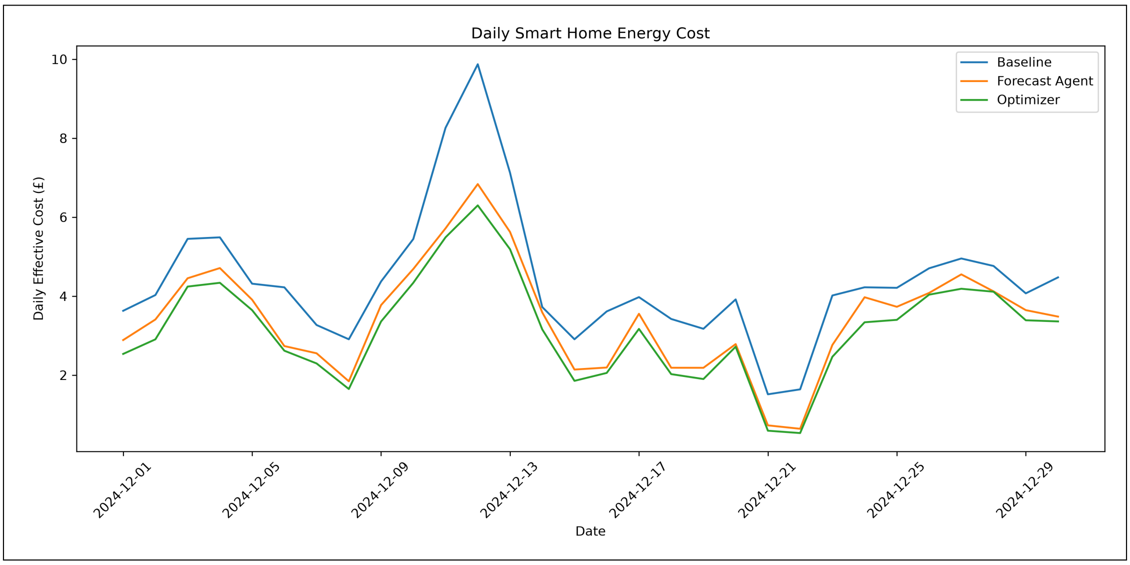

Figure 4. Daily effective cost by control strategy.

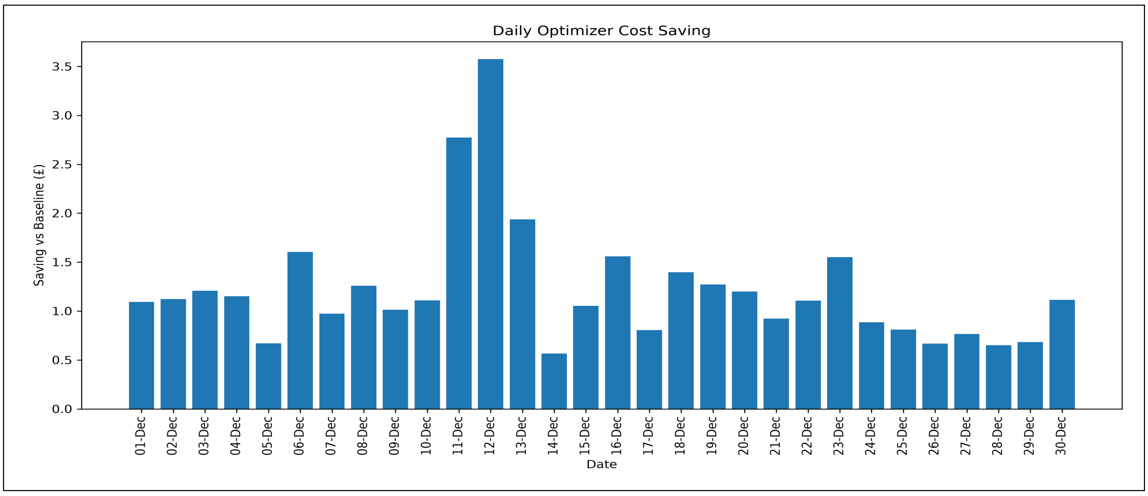

Figure 5. Daily MILP optimiser saving versus baseline.

5.3 Grid Import and Battery Behaviour

The important result that emerges in Figure 6 is that despite the fact that the MILP optimiser imported the greatest amount of energy from the grid (579.7 kWh) and the baseline imported the least (561.4 kWh), the optimiser was still 27.71% more cost-effective. Since there are inefficiencies of energy storage in a battery (that every 1 kWh of energy exported from the battery needs 1.108 kWh of energy to be purchased from the grid), cycling the battery results in a higher total import which, however, pays itself back due to the off-peak purchase of the energy.

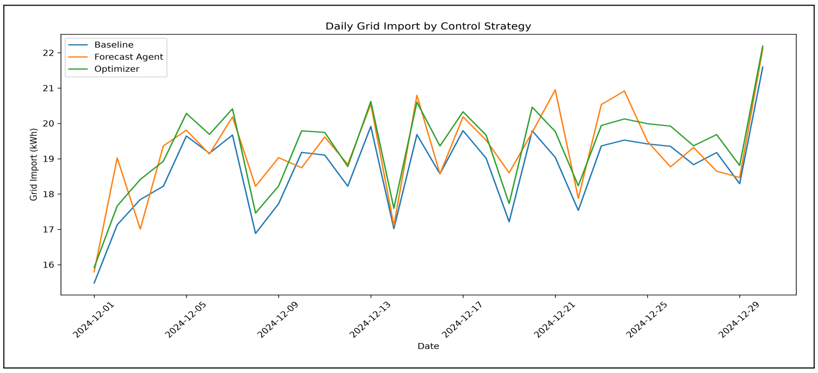

Figure 6. Daily grid import by control strategy.

As illustrated in Figure 7, the SOC evolution of the end of day is given. In the baseline, SOC never goes through a cycle and stays at zero for good. The forecast-based model, on the other hand, sometimes ends up with stranded energy (as much as 2.1 kWh) due to its threshold-based purchasing policy. The MILP optimiser, in contrast, almost always ends the day near-empty, holding energy overnight only when the day-ahead price structure justifies it, precisely the behaviour expected of a cost-optimal policy with a free terminal SOC. The final rise to 2.5 kWh on 30 December reflects the terminal condition of the last backtest day.

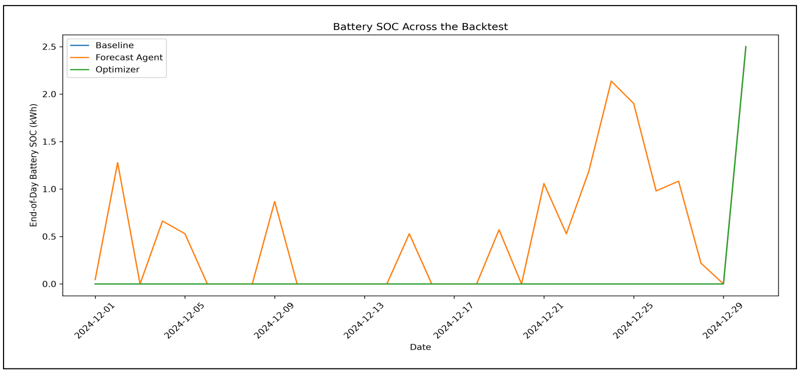

Figure 7. End-of-day battery state of charge across the backtest.

5.4 Sensitivity of the Agent's Thresholds

To assess how strongly the forecast-aware agent's performance depends on the selected thresholds (, ,) = (0.70, 1.40, 1.25), a one-at-a-time sensitivity experiment was conducted. Each threshold was varied over a wide range while the others were held at their selected values, and for every configuration the full 30-day simulation was re-run, carrying the SOC across days as in the main backtest. Because the study period's exact tariff series is consumed by the main experiment, the sensitivity runs use a 30-day synthetic Agile-like tariff ensemble statistically calibrated to the December 2024 backtest: it reproduces the diurnal trough–peak structure, day-to-day volatility including occasional spike days, and the mean realised import price of 23.44 p/kWh, while solar inputs are fixed to the thirty recorded daily generation totals distributed over the December daylight window and demand is unchanged. The calibration is validated by outcome: on this ensemble the agent with its selected thresholds saves 18.95% against the baseline, closely reproducing the 21.41% observed on the real data.

Table 5. Sensitivity analysis of the forecast-aware agent thresholds.

Threshold Varied	Range Tested	Cost Variation (% of Default)	Saving vs Baseline Across Range
Charge gate	0.60–0.80	10.1%	12.2%–20.4%
Spread ratio	1.20–1.60	$< 0.1\%$	19.0% throughout
Discharge gate	1.15–1.35	4.7%	16.0%–19.8%

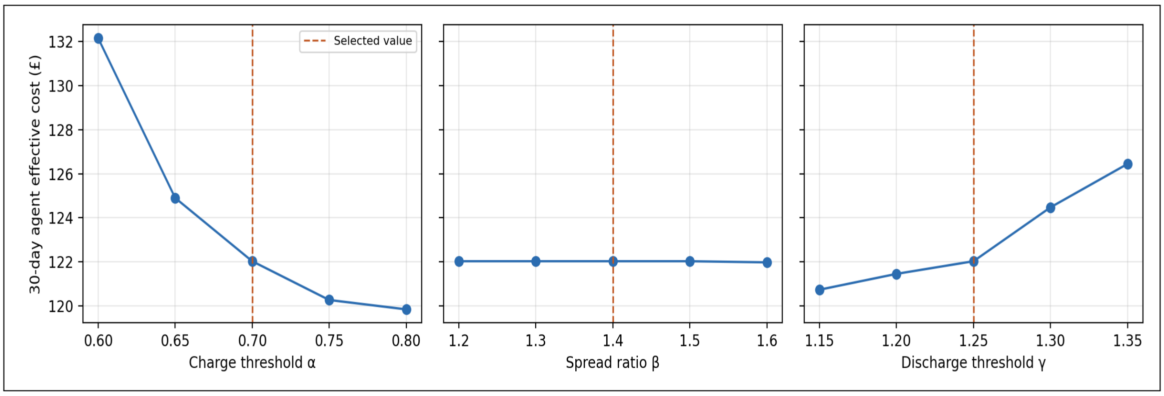

Figure 8. Threshold sensitivity of the forecast-aware agent (dashed lines mark the selected values).

Three observations follow from Table 5 and Figure 8. The agent outperforms the baseline under every tested configuration; the worst case across all fifteen configurations still saves 12.2%. The spread ratio is almost inert within the tested range because the charge gate already restricts purchases to deep price troughs where the spread condition is nearly always satisfied; functions as a safety guard that binds mainly on unusually flat days, consistent with its margin-above-breakeven role derived in Section 3.5. The selected values are near-optimal: relaxing to 0.80 improves the synthetic-ensemble cost by only 1.8%, at the price of more speculative purchases of the kind that produce the stranded-energy behaviour observed on the real data in Figure 7, and = 1.25 sits within 1.1% of the best tested value.

5.5 Discussion and Limitations

The gap between the forecast-aware agent (21.41%) and the MILP optimiser (27.71%) quantifies the value of exact optimisation over well-designed heuristics in this setting: the interpretable agent captures roughly 77% of the saving achieved by the MILP optimiser, at a fraction of the implementation complexity and with fully explainable decisions. This is a useful design point for commercial deployments where explainability and robustness to model error matter. Several limitations qualify the results. Household demand follows a deterministic stylised profile rather than measured smart-meter data. Both intelligent strategies enjoy perfect day-ahead knowledge of prices, which is realistic for Agile since day-ahead prices are published each afternoon, and of solar generation, which is optimistic since historical actuals stand in for forecasts. Solar export is modelled without a feed-in payment, understating potential revenue, and the degradation model is a linear throughput cost rather than an electrochemical ageing model. Finally, as justified in Section 4, the single-month December window is a deliberately adverse, low-solar stress scenario: the strategy ordering is expected to generalise, but annualised saving magnitudes and summer export economics remain to be quantified.

6. Conclusion and Future Work

The current research has introduced a smart home energy digital twin, based exclusively on actual UK tariffs and solar data. It was applied to benchmarking three autonomous control systems in equivalent scenarios, while considering the costs associated with batteries. Over a 30-day December 2024 backtest, the forecast-aware agent reduced household effective energy cost by 21.41% and the MILP optimiser by 27.71% relative to a static baseline, with the optimiser dominating on every single day. The agent's decision thresholds were derived analytically from battery arbitrage economics, and a sensitivity analysis confirmed that performance is robust across wide threshold ranges. The analysis further showed that under dynamic pricing the cost-optimal policy imports more energy, not less, monetising low-price windows through battery arbitrage and appliance shifting, and that intelligent control additionally reduces the volatility of the daily bill. Future work will proceed in four directions: (i) replacing perfect foresight with machine-learning forecasts of prices, solar generation, and demand, and quantifying the resulting optimality gap; (ii) extending the evaluation to a full-year backtest covering all seasons, together with sub-hourly satellite-derived irradiance to remove the hourly-to-half-hourly interpolation of Section 3.1; (iii) incorporating solar export tariffs, electric vehicle charging, and heat pump loads to reflect the fully electrified household; and (iv) closing the loop by deploying the MILP optimiser against physical hardware, with the digital twin retained online for anomaly detection and policy verification, and exploring reinforcement learning agents trained inside the twin as a bridge between the interpretability of rules and the optimality of mathematical programming.

References

[1] Grieves, Michael. "Digital Twin: Manufacturing Excellence Through Virtual Factory Replication." White Paper 1, 2014, no. 2014: 1-7.

[2] Tao, Fei, He Zhang, Ang Liu, and Andrew YC Nee. "Digital Twin in Industry: State-of-the-Art." IEEE Transactions on industrial informatics 2018, vol. 15, no. 4: 2405-2415.

[3] Semeraro, Concetta, Mario Lezoche, Hervé Panetto, and Michele Dassisti. "Digital Twin Paradigm: A Systematic Literature Review." Computers in Industry 2021, vol. 130: 103469.

[4] Beaudin, Marc, and Hamidreza Zareipour. "Home Energy Management Systems: A Review of Modelling and Complexity." Energy Solutions to Combat Global Warming (2016): 753-793.

[5] Zhou, Bin, Wentao Li, Ka Wing Chan, Yijia Cao, Yonghong Kuang, Xi Liu, and Xiong Wang. "Smart home Energy Management Systems: Concept, Configurations, and Scheduling Strategies." Renewable and Sustainable Energy Reviews 2016, vol. 6, 30-40.

[6] Mahapatra, Bandana, and Anand Nayyar. "Home Energy Management System (HEMS): Concept, Architecture, Infrastructure, Challenges and Energy Management Schemes: B. Mahapatra, A. Nayyar." Energy Systems 2022, vol. 13, no. 3: 643-669.

[7] Mohsenian-Rad, Amir-Hamed, and Alberto Leon-Garcia. "Optimal Residential Load Control with

Price Prediction in Real-Time Electricity Pricing Environments." IEEE Transactions on Smart Grid 1, 2010, no. 2: 120-133.

[8] Chen, Zhi, Lei Wu, and Yong Fu. "Real-Time Price-based Demand Response Management for Residential Appliances via Stochastic Optimization and Robust Optimization." IEEE transactions on smart grid 3, 2012, no. 4: 1822-1831.

[9] Sou, Kin Cheong, James Weimer, Henrik Sandberg, and Karl Henrik Johansson. "Scheduling Smart Home Appliances using Mixed Integer Linear Programming." In 50th IEEE conference on decision and control and European control conference, IEEE, 2011, 5144-5149.

[10] O'Neill, Daniel, Marco Levorato, Andrea Goldsmith, and Urbashi Mitra. "Residential demand response using reinforcement learning." In First IEEE international conference on smart grid communications, IEEE, 2010, 409-414.

[11] Vázquez-Canteli, José R., and Zoltán Nagy. "Reinforcement Learning for Demand Response: A Review of Algorithms and Modeling Techniques." Applied energy 2019, vol. 235, 1072-1089.

[12] Yu, Liang, Weiwei Xie, Di Xie, Yulong Zou, Dengyin Zhang, Zhixin Sun, Linghua Zhang, Yue Zhang, and Tao Jiang. "Deep Reinforcement Learning for Smart Home Energy Management." IEEE Internet of Things Journal 2019, vol. 7, no. 4: 2751-2762.

[13] Agostinelli, Sofia, Fabrizio Cumo, Giambattista Guidi, and Claudio Tomazzoli. "Cyber-Physical Systems Improving Building Energy Management: Digital Twin and Artificial Intelligence." Energies 2021, vol. 14, no. 8: 2338.

[14] Onile, Abiodun E., Ram Machlev, Eduard Petlenkov, Yoash Levron, and Juri Belikov. "Uses of the Digital Twins Concept for Energy Services, Intelligent Recommendation Systems, and Demand Side Management: A Review." Energy Reports 2021, vol. 7: 997-1015.

[15] O'Dwyer, Edward, Indranil Pan, Salvador Acha, and Nilay Shah. "Smart Energy Systems for Sustainable Smart Cities: Current Developments, Trends and Future Directions." Applied energy 2019, vol. 237: 581-597.

[16] Mitchell, Stuart, Michael OSullivan, and Iain Dunning. "Pulp: a Linear Programming Toolkit for Python." The University of Auckland, Auckland, New Zealand, 2011, vol. 65, no. 25: 1-12.

[17] Octopus Energy, "Agile Octopus Product and Public REST API Documentation," [Online]. Available: https://developer.octopus.energy/ (accessed January 2026).

[18] Open-Meteo, "Historical Weather API," [Online]. Available: https://open-meteo.com/ (accessed January 2026).